Burset Atienza, Pablo; Lu, Bo; Tamura, Shun; Tanaka, Yukio

Current fluctuations in unconventional superconductor junctions with impurity scattering

Published in:
Physical Review B

DOI:
10.1103/PhysRevB.95.224502

Published: 05/06/2017

Document Version
Publisher's PDF, also known as Version of record

PHYSICAL REVIEW B **95**, 224502 (2017)

Current fluctuations in unconventional superconductor junctions with impurity scattering

Pablo Burset,[1,2,3] Bo Lu,[2,4] Shun Tamura,[2] and Yukio Tanaka[2]
[1]*Institute for Theoretical Physics and Astrophysics, University of Würzburg, D-97074 Würzburg, Germany*
[2]*Department of Applied Physics, Nagoya University, Nagoya 464-8603, Japan*
[3]*Department of Applied Physics, Aalto University, FIN-00076 Aalto, Finland*
[4]*National Graphene Institute, University of Manchester, Booth St E, M13 9PL Manchester, United Kingdom*
(Received 13 March 2017; published 5 June 2017)

The order parameter of bulk two-dimensional superconductors is classified as *nodal* if it vanishes for a direction in momentum space, or *gapful* if it does not. Each class can be topologically nontrivial if Andreev bound states are formed at the edges of the superconductor. Nonmagnetic impurities in the superconductor affect the formation of Andreev bound states and can drastically change the tunneling spectra for small voltages. Here, we investigate the mean current and its fluctuations for two-dimensional tunnel junctions between normal-metal and unconventional superconductors by solving the quasiclassical Eilenberger equation self-consistently, including the presence of nonmagnetic impurities in the superconductor. As the impurity strength increases, we find that superconductivity is suppressed for almost all order parameters since (i) at zero applied bias, the effective transferred charge calculated from the noise-current ratio tends to the electron charge e, and (ii) for finite bias, the current-voltage characteristics follows that of a normal-state junction. There are notable exceptions to this trend. First, gapful nontrivial (chiral) superconductors are very robust against impurity scattering due to the linear dispersion relation of their surface Andreev bound states. Second, for nodal nontrivial superconductors, only p_x-wave pairing is almost immune to the presence of impurities due to the emergence of odd-frequency s-wave Cooper pairs near the interface. Due to their anisotropic dependence on the wave vector, impurity scattering is an effective pair-breaking mechanism for the remaining nodal superconductors. All these behaviors are neatly captured by the noise-current ratio, providing a useful guide to find experimental signatures for unconventional superconductivity.

DOI: 10.1103/PhysRevB.95.224502

I. INTRODUCTION

The symmetry of the superconducting order parameter is crucial to determine many properties of a superconductor. The majority of superconductors feature a conventional spin-singlet s-wave pair potential. Any deviation from this pair potential, be it spin-triplet states or higher harmonics such as a p-wave or a d-wave, is considered unconventional [1]. One of the most interesting consequences of unconventional pairings is the formation of surface Andreev bound states (SABSs) when the pair potential changes sign on the Fermi surface [2–6]. The formation of SABSs is related with the emergence of a zero bias peak (ZBP) in the tunnel conductance [5,6]. While conventional s-wave pairing is robust against nonmagnetic impurities [7], many unconventional pairings are fragile due to their anisotropic dependence on the wave vector [8]. Some SABSs have a topological origin and would be protected against imperfections or impurities [9–14]. However, impurity scattering reduces or completely suppresses the ZBP for many cases, making it difficult to detect unconventional pairing symmetries from conductance measurements only [15]. To go beyond dc conductance, it is interesting to study the nonequilibrium current fluctuations or shot noise [16]. The shot noise reveals the effective charge transferred in a given tunneling process through the noise-current ratio. For example, the effective charge of a tunnel junction between a normal metal and a superconductor is doubled, revealing the uncorrelated transfer of Cooper pairs due to Andreev processes [17–19].

In this work, we study the current, shot noise, and noise-current ratio of normal-metal–superconductor junctions, including the effect of nonmagnetic impurity scattering in the superconductor, for the most representative two-dimensional unconventional order parameters. We find that the noise-current ratio is a very useful tool to determine the type of superconducting pairing, even in the presence of impurity scattering. Depending on the shape of the order parameter in reciprocal space, superconductors in two dimensions can be classified into two groups: (i) gapful superconductors with a finite order parameter, and (ii) nodal superconductors where the order parameter vanishes in a given direction. At the same time, each order parameter can be topologically nontrivial or trivial depending on whether SABSs appear or not. For example, the conventional spin-singlet s-wave state belongs to the *gapful trivial* group. Chiral superconductors [20] are also gapped in the bulk, but they feature SABSs with a linear dispersion relation, thus they belong to the *gapful nontrivial* group. Sr_2RuO_4 is a strong candidate for a chiral spin-triplet p-wave superconductor [21]. Experiments have failed to detect the predicted spontaneous edge current in Sr_2RuO_4, suggesting that the chiral symmetry could be on a higher harmonic, such as a d- or f-wave [22]. Chiral pairing states have also been proposed for other systems, including graphene [23]. Chiral superconductors are currently attracting a lot of attention since their topologically nontrivial edge states, which display a linear dependence on the momentum, are a condensed-matter realization of Majorana states [24–26]. On the other hand, nodal superconductors with a vanishing order parameter feature SABSs with a flat dispersion relation at their edges [27]. Nodal superconductivity naturally appears in high-T_c cuprates [5,6,27] (d-wave) and noncentrosymmetric superconductors [28]. It can also be engineered by proximity effect from a conventional superconductor in materials with strong spin-orbit coupling [29,30] (p-wave). Assuming that the junction lies along the x direction, *nodal trivial* groups include

p_y- and $d_{x^2-y^2}$-waves, while *nodal nontrivial* correspond to p_x, d_{xy}, and similar.[1]

This paper is organized as follows. We describe our model and present the main definitions for the transport observables in Sec. II. In Sec. III, we present an exhaustive collection of transport results for ballistic junctions with unconventional superconductors. Here, our model reproduces many well-known results from previous works, and we discuss the most representative behavior of the different pairing symmetries. Next, in Sec. IV we show the main results of this work as we discuss the effect of impurities on the current, shot noise, and noise-current ratio of unconventional superconductors. We report our conclusions in Sec. V.

II. MODEL

We consider a two-dimensional normal-metal–superconductor junction where transport takes place along the x direction, and we set the interface at $x=0$. We thus parametrize the conserved transverse component of the wave vector k_y using the angle of incidence $\theta=\sin^{-1}(k_y/k_F)$, with k_F the Fermi wave vector. Depending on the direction of propagation of the quasiparticles, we define the angles $\theta_+\equiv\theta\in[-\pi/2,\pi/2]$ and $\theta_-=\pi-\theta$. We model the scattering at the interface using a δ-function potential $V(x)=Z(\hbar^2k_F/2m)\delta(x)$, with Z the dimensionless barrier strength and m the electron mass. We assume a clean normal metal $(x<0)$ and a uniform distribution of nonmagnetic impurities in the superconducting region $(x>0)$ with induced self-energy $\hat{a}(x)$. The superconducting order parameter is given by $\hat{\Delta}(\theta_\alpha,x)$, with $\alpha=\pm$. In the normal region, we take $\hat{a}(x<0)=\hat{\Delta}(\theta_\alpha,x<0)=0$. For a spin-degenerate system, the quasiclassical Green's function [31–34] $\hat{g}^{\alpha\alpha}(i\omega_n,\theta_\alpha,x)$ for Matsubara frequency $\omega_n=(2n+1)\pi T$, where T is the temperature and n is an integer, is a 2×2 matrix in particle-hole space that satisfies the Eilenberger equation [35]

$$i v_{Fx}\partial_x\hat{g}^{\alpha\alpha}+\alpha[i\omega_n\hat{\tau}_3-\hat{\Delta}(\theta_\alpha,x)\hat{\tau}_3-\hat{a}(x),\hat{g}^{\alpha\alpha}]=0. \quad (1)$$

Here, $v_{Fx}=v_F\cos\theta$ is the x component of the Fermi velocity v_F, and the particle-hole space is spanned by Pauli matrices $\hat{\tau}_{0,1,2,3}$, with $\hat{\tau}_0$ the identity matrix. The quasiclassical Green's function is normalized as $(\hat{g}^{\alpha\alpha})^2=-1$.

To account for unconventional superconductivity in the rightmost region $(x>0)$, we use the notation

$$\hat{\Delta}(\theta_\alpha,x)\equiv[\Delta_R(x)\chi_R(\theta_\alpha)\hat{\tau}_1-\Delta_I(x)\chi_I(\theta_\alpha)\hat{\tau}_2]\Theta(x), \quad (2)$$

with $\Theta(x)$ the Heaviside function. The subindices R,I refer to the real or imaginary part of the order parameter. We choose the global $U(1)$ gauge so that the order parameter is real for nonchiral superconductors or it is proportional to a cosine function of the angle for chiral ones. The resulting form factors $\chi_{R,I}(\theta_\alpha)$ are enumerated in Table I.

The spatial dependence of the order parameter is determined self-consistently in terms of the quasiclassical Green's function, namely [15,36]

$$\Delta_R(x)=\frac{2T\sum_{n\geqslant0}\langle\langle\chi_R(\theta_\alpha)[\hat{g}^{\alpha\alpha}(\omega_n,\theta_\alpha,x)]_{12}\rangle\rangle_\theta}{\ln\frac{T}{T_c}+\sum_{n>0}\frac{1}{n-1/2}}, \quad (3)$$

$$\Delta_I(x)=-i\frac{2T\sum_{n\geqslant0}\langle\langle\chi_I(\theta_\alpha)[\hat{g}^{\alpha\alpha}(\omega_n,\theta_\alpha,x)]_{12}\rangle\rangle_\theta}{\ln\frac{T}{T_c}+\sum_{n>0}\frac{1}{n-1/2}}, \quad (4)$$

with the angle average defined as $\langle\langle f(\theta_\alpha)\rangle\rangle_\theta=\sum_\alpha\int_{-\pi/2}^{\pi/2}d\theta\, f(\theta_\alpha)$. The sums include a cutoff $n_{\max}$, defined as the maximum integer that satisfies $n_{\max}\leqslant\omega_D/(2\pi T)$. T_c is the critical temperature of the bulk superconductor and $\omega_D=2\pi T_c$ is the Debye frequency, ignoring thermodynamic phenomena. In the bulk of the superconductor, i.e., deep inside the superconducting region, a finite order parameter fulfills $\Delta_{R,I}(x\to\infty)\equiv\Delta_b$.

Following Ref. [15], the self-energy for the distribution of nonmagnetic impurities is written as $\hat{a}=\sum_{j=1}^3 a_j\hat{\tau}_j$, with

$$a_j(\omega_n,x)=\frac{\frac{-1}{2\tau}\frac{1}{1-\sigma}\left\langle\!\left\langle g_j^{\alpha\alpha}(\omega_n,x)\right\rangle\!\right\rangle_\theta}{1-\frac{1}{1-\sigma}\sum_j\left[\left\langle\!\left\langle g_j^{\alpha\alpha}(\omega_n,x)\right\rangle\!\right\rangle_\theta\right]^2}, \quad (5)$$

where $1/\tau$ and σ are the normal scattering rate and the strength of a single impurity potential, respectively.

For the numerical calculations, it is useful to express the Green's function in terms of the Riccati parameters [37–39] as

$$\hat{g}^{\alpha\alpha}=\frac{i\alpha}{1-\mathcal{G}_\alpha^S\mathcal{F}_\alpha^S}\begin{bmatrix}1+\mathcal{G}_\alpha^S\mathcal{F}_\alpha^S & 2i\mathcal{F}_\alpha^S\\ 2i\mathcal{G}_\alpha^S & -1-\mathcal{G}_\alpha^S\mathcal{F}_\alpha^S\end{bmatrix}, \quad (6)$$

where $\mathcal{G}_\alpha^S(\omega_n,\theta_\alpha,x)$ and $\mathcal{F}_\alpha^S(\omega_n,\theta_\alpha,x)$ satisfy the equations

$$\alpha v_{Fx}\partial_x\mathcal{G}_\alpha^S=2(\omega_n-ia_3)\mathcal{G}_\alpha^S+\Lambda_1^\alpha\left(\mathcal{G}_\alpha^S\right)^2-\Lambda_2^\alpha, \quad (7)$$

$$\alpha v_{Fx}\partial_x\mathcal{F}_\alpha^S=-2(\omega_n-ia_3)\mathcal{F}_\alpha^S+\Lambda_2^\alpha\left(\mathcal{F}_\alpha^S\right)^2-\Lambda_1^\alpha, \quad (8)$$

with

$$\Lambda_{1,2}^\alpha=\Delta_R\chi_R(\theta_\alpha)+ia_2\pm i[\Delta_I\chi_I(\theta_\alpha)+ia_1]. \quad (9)$$

Finally, at the interface, we set the boundary conditions [40–44]

$$\mathcal{F}_\alpha^S(x=0)\to\frac{(1-\sigma_{n\theta})^{\alpha\,\mathrm{sgn}(\omega_n)}}{\mathcal{G}_{-\alpha}^S(x=0)}, \quad (10)$$

with $\sigma_{n\theta}=4\cos^2\theta/(Z^2+4\cos^2\theta)$ the normal-state angle-dependent transmission.

Following the scattering formalism [45], the Andreev (a) and normal (b) reflection amplitudes at the interface are given by

$$a=\frac{i\bar{\mathcal{G}}_+^S}{1+\sigma_{n\theta}(1-\bar{\mathcal{G}}_+^S/\bar{\mathcal{G}}_-^S)}, \quad (11)$$

$$b=\frac{Z}{2i\cos\theta-Z}\frac{\frac{1}{\sigma_{n\theta}}(1-\bar{\mathcal{G}}_+^S/\bar{\mathcal{G}}_-^S)}{1+\sigma_{n\theta}(1-\bar{\mathcal{G}}_+^S/\bar{\mathcal{G}}_-^S)}, \quad (12)$$

with $\bar{\mathcal{G}}_\alpha^S=\mathcal{G}_\alpha^S(E,\theta_\alpha,x=0)$ and $E>0$ the real excitation energy of an incident quasiparticle.

[1] We are considering the situation in which the nodal direction lies along the x direction. In a more general case, there can be an angle between the nodal direction and the x axis. A slightly tilted p_y-wave or $d_{x^2-y^2}$-wave pairing is then nontrivial, but it will behave in a similar way as the trivial cases studied here. We are only interested in the representative behavior for two-dimensional superconductors, so we will not consider such cases here.

TABLE I. Symmetry of the superconducting pairing, transport results for $E = 0$ and $Z = 5$, and excess current. The symbol ✓ (×) represents "presence of ..." ("absence of ..."). Zero-bias peak (ZBP) indicates the case in which $\sigma_S \gg \sigma_N$. Results in the ballistic (bal.) and impurity regimes are taken with $1/(2\tau\Delta_b) = 0$ and 0.2, respectively. Born (B) and unitary (U) limits are calculated with $\sigma = 0$ and $\sigma = 0.99$, respectively.

						σ_S/σ_N		P_S/S_N		$P_S/(2e\sigma_S)$		I_{exc}	
Type	wave	$\chi_R(\theta_\pm)$	$\chi_I(\theta_\pm)$	node	SABS	bal.	impurity	bal.	impurity	bal.	impurity	bal.	impurity
1. Gapful trivial	s	1	0	×	×	$\to 0$	$\to 0$	$\to 0$	$\to 0$	2	$\to 1$	0	0
2. Gapful nontrivial	chiral-p (χ_p)	$\pm\cos\theta$	$\sin\theta$	×	linear	~ 1	~ 1	~ 1	~ 1	$\lesssim 1$	~ 1	0	0
	chiral-d (χ_d)	$\cos 2\theta$	$\pm\sin 2\theta$	×	linear	$\sim 1/2$	$\gtrsim 1/2$	$\sim 1/2$	$\sim 1/2$	$\gtrsim 1$	~ 1	0	0
	chiral-f (χ_f)	$\pm\cos 3\theta$	$\sin 3\theta$	×	linear	$\sim 1/2$	$\gtrsim 1/2$	$\sim 1/2$	$\sim 1/2$	$\gtrsim 1$	~ 1	0	0
3. Nodal trivial	p_y	$\sin\theta$	0	✓	×	> 0	$\sim 1/10\,(B)$	$\ll 1$	$\ll 1\,(B)$	~ 2	$\gtrsim 3/2\,(B)$	0	0
							$\sim 1/2\,(U)$		$\sim 1/2\,(U)$		$\sim 1\,(U)$		
	$d_{x^2-y^2}$	$\cos 2\theta$	0	✓	×	> 0	$\gtrsim 1/10\,(B)$	$\ll 1$	$\ll 1\,(B)$	$\lesssim 2$	$\lesssim 2\,(B)$	0	0
							$\sim 1/2\,(U)$		$\sim 1/2\,(U)$		$\sim 1\,(U)$		
4. Nodal nontrivial	p_x	$\pm\cos\theta$	0	✓	flat	ZBP	ZBP	0	0	0	0	$I_{\text{exc}}^{\text{ball}}$	$I_{\text{exc}}^{\text{ball}}$
	d_{xy}	$\pm\sin 2\theta$	0	✓	flat	ZBP	~ 2	0	$\sim 3/2$	0	$\lesssim 1$	$I_{\text{exc}}^{\text{ball}}$	$\to 0$
	f_x	$\pm\cos 3\theta$	0	✓	flat	ZBP	~ 2	0	$\sim 3/2$	0	$\lesssim 1$	$I_{\text{exc}}^{\text{ball}}$	$\to 0$

Using the reflection amplitudes, we define the differential conductance [5,6]

$$\sigma_S(E) = \frac{2e^2}{h}\int_{-\pi/2}^{\pi/2} d\theta\cos\theta(1 - |b|^2 + |a|^2), \tag{13}$$

and differential noise power [18]

$$P_S(E) = \frac{4e^3}{h}\int_{-\pi/2}^{\pi/2} d\theta\cos\theta[|a|^2(1-|a|^2) + |b|^2(1-|b|^2) + 2|a|^2|b|^2]. \tag{14}$$

In the normal state, the differential conductance and noise power are defined, respectively, as

$$\sigma_N = R_N^{-1} = \frac{e^2}{h}\int_{-\pi/2}^{\pi/2} d\theta\cos\theta\sigma_{n\theta},$$

$$S_N = \frac{2e^3}{h}\int_{-\pi/2}^{\pi/2} d\theta\cos\theta\sigma_{n\theta}(1-\sigma_{n\theta}).$$

The zero-temperature current and shot noise are then obtained integrating Eqs. (13) and (14) for a finite voltage, respectively,

$$I_S(eV) = \int_0^{eV}\sigma_S(E)dE, \tag{15}$$

$$S_S(eV) = \int_0^{eV} P_S(E)dE, \tag{16}$$

with V the voltage drop at the NS interface.[2]

III. BALLISTIC JUNCTION

In this section, we use our model for the study of ballistic (impurity-free) normal-metal–superconductor junctions with a barrier controlling the interface transmission. The following results for conductance, shot noise, and noise-current ratio are gathered in Table I under the columns "ballistic."

In the limit of transparent junction, with $Z = 0$, all types of superconductors feature a perfect Andreev reflection at the interface. Consequently, the differential conductance is a constant with twice the value of the normal-state conductance for small applied bias voltage compared to the bulk gap [see Fig. 1(a)]. To clearly distinguish between the different types of superconductor, one must make use of the tunnel conductance, opening the possibility of normal backscattering at the interface. As we approach the tunnel limit, $Z \gg 1$, the zero-energy conductance for each type of superconductor becomes different featuring three illustrative behaviors.

Nodal nontrivial superconductors, with p_x-, d_{xy}-, or f_x-wave symmetry, feature a perfect Andreev reflection independently of the barrier strength. Since the normal-state conductance is reduced by increasing Z, the normalized tunnel conductance σ_S/σ_N prominently displays a zero-bias peak.

For gapful nontrivial (chiral) superconductors, the conductance reduces to a finite value, slightly over σ_N for the chiral p-wave case or comparable to $\sigma_N/2$ for the rest of the chiral pairing states.

For trivial superconductors, both nodal and gapful, the conductance is reduced well below the normal-state conductance σ_N. The resulting normalized tunnel conductance is strongly suppressed for small energies, featuring a (U-) V-shaped profile for (gapful) nodal pairing states. In the gapful trivial case the conductance tends to zero, while for the nodal trivial cases it tends to a finite but small value [15].

The tunnel conductance in the ballistic limit is thus a useful tool to explore the symmetry of the superconducting pairing. However, the height of the zero-bias peak and the gap suppression are very sensitive to the barrier strength and are also rounded by temperature effects [15]. Therefore, tunnel conductance experiments can sometimes be ambiguous. Charge fluctuations of the current provide an extra layer of information on the symmetry of the pairing potential. For a ballistic junction, the noise power at zero temperature can also be interpreted in terms of the reflection processes only [17,18]. For energies below the gap, the integrand of

[2] In the self-consistent evaluation of the pairing states, we have not included thermodynamic phenomena. Accordingly, in the numerical calculations, we choose a sufficiently small temperature $T = 0.05T_c$.

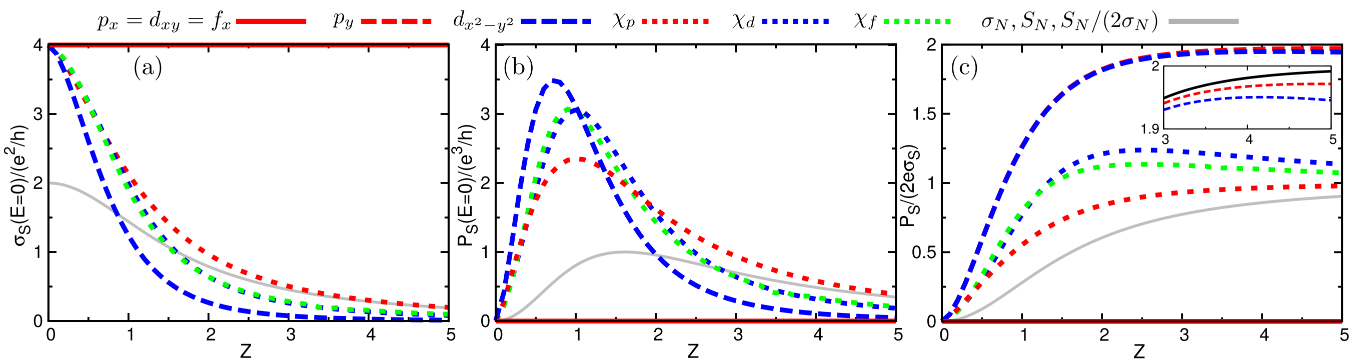

FIG. 1. Transport results without impurities. Zero-bias differential conductance (a), noise power (b), and their ratio (c) as a function of the barrier strength Z for different unconventional pairing symmetries. The gray lines show the corresponding results for a junction in the normal state. The inset in (c) compares p_y- and $d_{x^2-y^2}$-wave symmetries with the s-wave case (black solid line). Chiral p, d, and f symmetries are denoted as $\chi_{p,d,f}$, respectively.

Eq. (14) reduces to $4|a|^2(1-|a|^2)$. Consequently, for perfect Andreev reflection ($|a|^2=1$) or in the absence of it ($|a|^2=0$), the noise power is zero. Therefore, nodal nontrivial superconductors are always noiseless at zero energy independently of the barrier strength [46,47], as shown in Fig. 1(b). The noise power for the rest of the pairing states develops a maximum between the transparent and tunnel limits. The maxima for each pairing occur for different values of the barrier strength. However, it would be pointless to use this to experimentally identify each symmetry since the barrier Z is a fitting parameter that accounts for many possible sources of interfacial scattering [45].

A more clear distinction between all superconductors is given by the noise-current ratio, shown in Fig. 1(c), which determines the effective charge transferred at the interface. Since nodal nontrivial superconductors are noiseless independently of the barrier strength, their ratio is also zero. Gapped nontrivial (chiral) superconductors have an effective charge equal to the electron charge in the tunnel limit [47]. In this case, the conducting channels are a superposition of modes with a strong Andreev reflection amplitude (i.e., those with angle of incidence $|\theta|\gtrsim 0$ that feature a linear SABS) and others with strong normal backscattering (for $|\theta|\lesssim\pi/2$). For trivial superconductors, gapful or nodal, the effective transferred charge approaches $2e$ in the tunnel regime, indicating the transfer of a Cooper pair at the junction. Small differences between s-, p_y-, and $d_{x^2-y^2}$-wave superconductors appear in the tunnel limit, as shown in the inset of Fig. 1(c). However, they do not affect the general behavior of the ratio.

In summary, there are three general trends for ballistic junctions that are neatly captured in the noise-current ratio in the tunnel limit: (i) Nodal nontrivial superconductors display a noiseless zero-bias peak and their ratio is zero; (ii) chiral superconductors feature a conductance of magnitude comparable to the normal state with noise-current ratio 1; and (iii) trivial (gapful and nodal) superconductors have a suppressed conductance and ratio approaching 2.

IV. IMPURITY SCATTERING IN THE SUPERCONDUCTOR

We now consider the presence of nonmagnetic impurities in the superconductor. We explore two cases for the impurity potential. The Born limit accounts for weak impurity potentials that induce small scattering phase shifts. We thus take the limit $\sigma\to 0$ in Eq. (5) and find

$$\hat{a}\sim-\frac{1}{2\tau}\left\langle\!\left\langle\sum_j g_j^{\alpha\alpha}\hat{\tau}_j\right\rangle\!\right\rangle_\theta. \tag{17a}$$

On the other hand, the unitary limit considers infinitely strong impurity potentials. Taking $\sigma\to 1$ in Eq. (5) results in

$$\hat{a}\sim\frac{1}{2\tau}\frac{1}{\langle\langle\sum_j g_j^{\alpha\alpha}\hat{\tau}_j\rangle\rangle_\theta}. \tag{17b}$$

In the bulk of the superconductor, the Green's function becomes divergent for energies close to the continuum levels at the edges of the gap. Close to the interface, however, the Green's function can develop divergences in the presence of emergent SABS and it is approximately zero otherwise. The impact of the impurity scattering is determined crucially by whether the superconductor is nontrivial and develops SABS or is trivial and does not have subgap states [15]. For nontrivial superconductors, given a fixed scattering rate $1/\tau$, the self-energy $\hat{a}$ diverges in the Born limit and is greatly suppressed in the unitary limit. For trivial superconductors we expect the opposite behavior.

In the following, we set the barrier strength $Z=5$, where the general behavior of trivial and nontrivial unconventional superconducting orders is clearly displayed, and we study the effect of scattering by nonmagnetic impurities in the superconductor for zero and finite applied bias.

A. Effect of impurities at zero bias

The zero-bias transport results, for a tunnel junction with $Z=5$, are shown in Fig. 2(a) for the Born limit and in Fig. 2(b) for the unitary one. In both cases, we immediately observe a different behavior between the p_x-wave and the rest of the nodal nontrivial states. For the moderate impurity scattering rates considered in this work, p_x-wave superconductors are immune to the effect of nonmagnetic impurities. The ballistic zero-bias noiseless conductance is unaltered in the Born and unitary limits. Conversely, for the d_{xy}- and f_x-wave cases, the zero-bias conductance peak is reduced by the impurity potential. As the impurity strength is increased, conductance

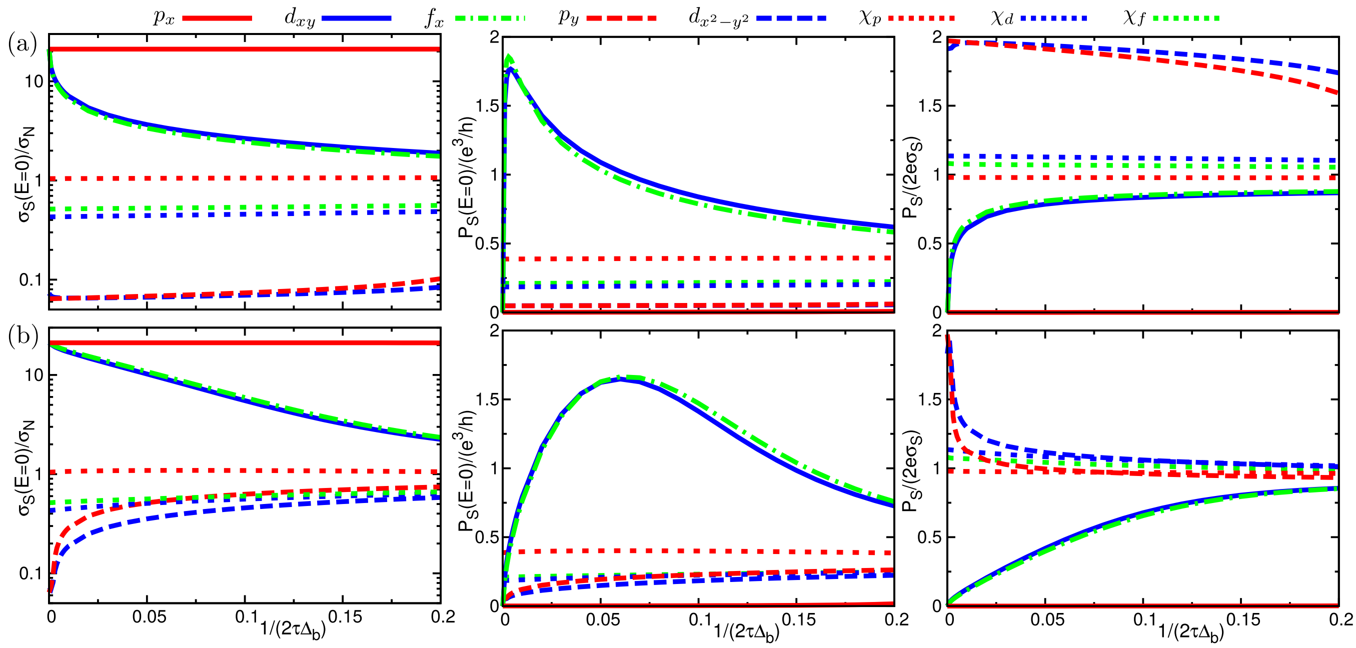

FIG. 2. From left to right, differential conductance, noise power, and their ratio for $E = 0$ as a function of the impurity scattering rate $1/\tau$ normalized to the bulk gap Δ_b. In the left panels, the conductance is normalized to the normal-state value. (a) Born limit with $\sigma = 0$. (b) Unitary limit with $\sigma = 0.99$. In all cases, $Z = 5$. Chiral p, d, and f symmetries are denoted as $\chi_{p,d,f}$, respectively.

and shot noise tend to the same value, with the ratio equal to 1. It is interesting to note that the noise power for these superconductors, which is zero in the ballistic limit, develops a maximum as a function of the scattering rate $1/\tau$, similarly to the barrier dependence in the ballistic limit for the rest of the superconductors. Nodal trivial superconductors, like the p_y- and $d_{x^2-y^2}$-wave cases, are also strongly modified by impurities. In the unitary limit, the conductance and shot noise of these superconductors are increased at zero bias, with a clear tendency toward the normal-state case. A similar trend is observed in the Born limit, although the evolution with the scattering rate is very smooth. By looking at the noise-current ratio, this tendency becomes evident for both the Born and unitary limits (rightmost panels of Fig. 2). The ratio is reduced from 2 to 1 for trivial pairings, and it is increased from 0 to 1 for nontrivial ones, with the notable exception being the p_x-wave. As expected from Eq. (17), this transition is faster in the Born limit than in the unitary one for nontrivial superconductors, while trivial pairings follow the opposite behavior.

The special case of p_x-wave pairing can be explained by the emergence of isotropic odd-frequency Cooper pairs at the interface [36,48]. Inhomogeneous superconducting systems feature a ubiquitous presence of odd-frequency pairing [49–53], where the wave function of Cooper pairs is odd under the exchange of the time coordinates of the electrons forming it [14,54,55]. In the ballistic limit, the noiseless zero-bias conductance peak of nodal nontrivial superconductors is formed due to a dominant odd-frequency pairing state near the interface [15]. To fulfill Fermi-Dirac statistics, these Cooper pairs form an s-wave state for p_x-wave superconductors or a p-wave state (d-wave) for d_{xy}-wave (f_x-wave) superconductors. The presence of impurities suppresses all the anisotropic pairing states, and only p_x-wave order maintains the ballistic result.

Finally, chiral superconductors are mostly unaffected by the impurity scattering. This behavior is clearly shown by the noise-current ratio, which remains almost 1 in both the Born and unitary limits for several values of the scattering rate. At first glance, this result seems at odds with the fact that nontrivial superconductors should be sensitive to impurity scattering in the Born limit. The main difference is that gapful nontrivial superconductors feature SABSs with a linear dispersion relation, instead of flat bands like nodal superconductors. The resulting angle-averaged Green's function at low energies for chiral superconductors is not divergent, since the SABSs only contribute for specific values of the angle (e.g., for $E = 0$, the chiral p-wave SABS has a small contribution at $|\theta| \sim 0$). This fundamental difference justifies the importance of chiral superconductors as sources of SABSs with topological protection against disorder [20,56].

B. Effect of impurities at finite bias

We now study the voltage dependence of the current and fluctuations. In the normal state, the current through the junction follows a linear Ohmic behavior where $I_N = R_N^{-1} V$, with R_N the normal-state resistance and V the applied voltage (see the gray lines in Fig. 3). In the superconducting state, the current is drastically changed for bias values comparable to the superconducting gap Δ_b. The I-V curves of conventional singlet s-wave normal-metal–superconductor junctions in the ballistic limit are well known; see, e.g., Refs. [45,57]. In the tunnel regime, the current is suppressed for voltages below the gap, while it is linear with slope R_N^{-1} for high voltages, $eV > \Delta_b$. This conventional behavior is qualitatively reproduced by nodal trivial superconductors with p_y- and $d_{x^2-y^2}$-wave symmetries. The main difference is a less pronounced suppression below the gap in the ballistic case;

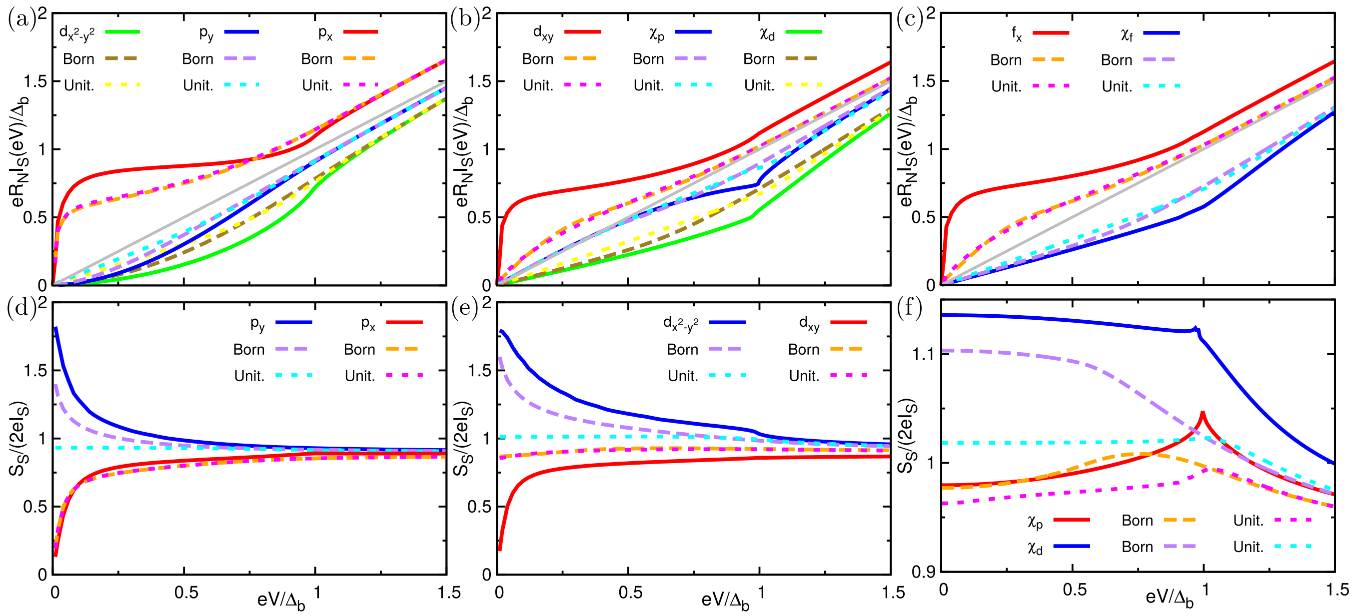

FIG. 3. Voltage dependence of the current (a)–(c) and noise-current ratio (d)–(f) for different pairing symmetries in the ballistic (solid lines), Born (dashed lines), and unitary (dotted lines) limits. The latter two are plotted for $1/(2\tau\Delta_b) = 0.2$. The gray line is the normal-state current. Chiral p, d, and f symmetries are denoted as $\chi_{p,d,f}$, respectively.

see the solid blue and green lines of Fig. 3(a). In the presence of impurities, the subgap suppression is even milder (dashed lines for the Born limit and dotted lines for the unitary limit).

Chiral p-wave superconductors [blue line in Fig. 3(b)] are clearly distinguished from the chiral d- and f-wave cases [green line in Fig. 3(b) and blue line in Fig. 3(c), respectively]. While chiral p-wave superconductors mostly follow an Ohmic behavior, with a small dip at $eV \sim \Delta_b$, the current for the other chiral waves is suppressed below I_N, even for voltages over the gap. The finite voltage current is thus helpful to distinguish chiral p-wave symmetry from d-wave or higher, which is qualitatively similar to trivial superconductors. The main effect of impurity scattering on chiral superconductors is to soften the dip at $eV \sim \Delta_b$, where the presence of continuum bands makes $\langle\langle\sum_j \hat{g}_j(E \sim \Delta_b, x = 0)\hat{\tau}_j\rangle\rangle_\theta$ diverge [15,58]. As a consequence, the self-energy is acutely increased in the Born limit, while it is suppressed in the unitary limit; cf., Eq. (17). The current dips, which are clearly distinguishable in the ballistic limit, can still be appreciated in the unitary limit but are completely suppressed in the Born limit.

Nodal nontrivial superconductors display a completely different behavior. Even in the tunnel regime considered here with $Z = 5$, the subgap current is greatly enhanced in the ballistic limit. The impurity scattering reduces the subgap contribution of d_{xy}- and f_x-wave superconductors, although the current is still greater than I_N. Conversely, the current for p_x-wave superconductors is enhanced over the Ohmic case even in the presence of impurities.

As for the zero-bias results, the noise-current ratio clearly displays the behavior of each pairing state, as is shown in Figs. 3(d)–3(f).[3] The Ohmic I-V curves for $eV > \Delta_b$ yield a ratio 1. For nodal trivial gaps, the ballistic, Born, and unitary limits present different ratios going from 2 (ballistic) to 1 (unitary). Nodal nontrivial pairings quickly approach the Ohmic limit in the presence of impurities, with the exception of the p_x-wave state. In Fig. 3(f) we compare the chiral p-wave and d-wave states (which also qualitatively represents the chiral f-wave state). The chiral p-wave is only slightly modified by impurities at finite voltage. At low voltage, the ratio is only slightly affected in the unitary limit. However, the rest of the chiral states are a bit more sensitive, although in a small scale.

To study the I-V characteristics at high voltages, we define the excess current as the difference between the superconducting and normal-state currents, namely

$$I_{\rm exc}(V) = I_S(eV) - I_N(eV). \tag{18}$$

The presence of a finite excess current for high voltages, ideally for $eV \to \infty$, indicates a strong contribution of Andreev reflections for energies below the gap [45,57,59–61]. In the ballistic limit, nodal nontrivial superconductors feature a finite excess current while it is suppressed for the rest of the superconductors at large voltages. The value of the maximum excess current is determined by the interface transparency, resulting in $I_{\rm exc}^{\rm ball}(Z = 5) \simeq (1/6)\Delta_b/(eR_N)$. In Fig. 4, we show the evolution of the excess current as a function of the impurity scattering rate, calculated at $eV = 2\Delta_b$. Negative values of $I_{\rm exc}(2\Delta_b)$ indicate that the excess current is suppressed for $eV \gg \Delta_b$. It is interesting that the presence of impurity scattering does not accelerate the transition into I_N for chiral or trivial superconductors. However, impurity scattering suppresses the excess current for nodal nontrivial superconductors, with the exception of the p_x-wave. Remarkably, p_x-wave superconductors maintain the ballistic result even in the presence of impurities, even though the excess current for the rest of the nodal nontrivial

[3]The noise-current ratio in Figs. 3(d)–3(f) is only well defined for finite voltage, since $I_S(V = 0) = 0$.

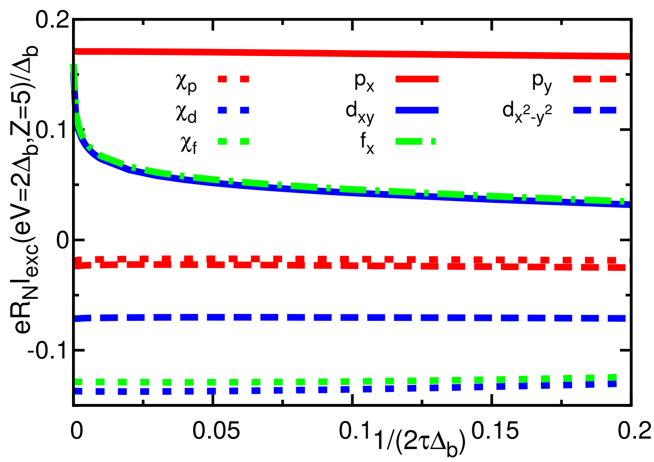

FIG. 4. In the Born limit with $1/(2\tau\Delta_b) = 0.2$, excess current for $eV = 2\Delta_b$ as a function of the impurity scattering rate. Chiral p, d, and f symmetries are denoted as $\chi_{p,d,f}$, respectively.

cases is reduced to the normal-state case. The presence of a noiseless perfect Andreev reflection in the zero-energy channel of p_x-wave superconductors is thus directly responsible for a finite excess current, even in the presence of impurities.

V. CONCLUSIONS

We present an exhaustive description of the transport properties of two-dimensional junctions with unconventional superconductors, including the effect of scattering by nonmagnetic impurities in the superconductor. The main results of this work are gathered in Table I. We have classified two-dimensional superconducting order parameters as gapful or nodal, where the latter vanishes for a particular direction of the wave vector. Each class can be topologically nontrivial if the superconductor features SABSs. The noise-current ratio is a perfect tool to identify each class in an impurity-free ballistic junction in the tunnel limit. Indeed, the ratio is zero for nodal nontrivial superconductors, 1 for gapful nontrivial ones, and 2 for trivial pairings, both nodal or gapful.

The inclusion of impurity scattering at the superconductor further distinguishes unconventional superconductors, and these changes are again clearly captured in the noise-current ratio. The ratio for trivial superconductors is decreased from 2 to 1 as the scattering rate is increased. This transition is faster in the unitary limit, and dominant in the absence of SABSs. Conversely, the ratio for nodal nontrivial superconductors is increased from 0 to 1, and the transition is faster in the Born limit. A notable exception is the case of a p_x-wave. This special nodal pairing develops an s-wave odd-frequency component at the interface that is highly resistant to impurity scattering. Interestingly, gapful nontrivial (chiral) superconductors are also resistant to the impurity scattering. The linear dispersion of the SABSs in these superconductors guarantees that the correction coming from the self-energy of the impurity distribution is always small. Their noise-current ratio is thus barely changed by the presence of nonmagnetic impurities, a clear signature of the topological protection of these pairing states.

Our results can be used for the experimental classification of pairing symmetries. We have demonstrated the utility of noise measurements for the identification of order parameters, even in the cases in which tunnel conductance can be ambiguous [62].

A special mention should be made about p_x-wave pairing. The flatband SABS of this nodal superconductor induces a perfect Andreev reflection, resulting in a noiseless resonance at zero energy. This behavior survives the presence of nonmagnetic impurities in the superconductor and can be observed even when the normal metal is in the diffusive regime [63]. The origin of this anomalous proximity effect is the formation of isotropic odd-frequency Cooper pairs at the interface [48]. Another manifestation of such an exotic odd-frequency Andreev resonance presented here is that the excess current maintains the ballistic maximum value in the presence of impurities, a feature unique to this pairing state. The special zero-energy state of p_x-wave superconductors is connected to the emergence of a Majorana bound state [64]. Indeed, Majorana states are always accompanied by odd-frequency Cooper pairs [65,66]. It is thus very motivating that a finite excess current has been recently reported in experiments to identify Majorana bound states in topological Josephson junctions [61].

Finally, the connection between symmetry of the pairing state and transport properties of two-dimensional spin-degenerate superconducting junctions presented here provides a good starting point to consider more complicated three-dimensional pairing states.

ACKNOWLEDGMENTS

The authors are grateful to Y. Asano for valuable discussions. P.B. acknowledges support from Japan Society for the Promotion of Science International Research Fellowship and the European Union's Horizon 2020 research and innovation programme under the Marie Skłodowska-Curie grant agreement No. 743884. B.L. acknowledges EPSRC Grant No. EP/N010345/1 and European Graphene Flagship Project. This work was also supported by a Grant-in-Aid for Scientific Research on Innovative Areas Topological Material Science JPSJ KAKENHI (Grants No. JP15H05851, No. JP15H05853, and No. JP15K21717), a Grant-in-Aid for Scientific Research B (Grant No. JP15H03686), and a Grant-in-Aid for Challenging Exploratory Research (Grant No. JP15K13498) from the Ministry of Education, Culture, Sports, Science, and Technology, Japan (MEXT).

[1] M. Sigrist and K. Ueda, Phenomenological theory of unconventional superconductivity, Rev. Mod. Phys. **63**, 239 (1991).
[2] L. J. Buchholtz and G. Zwicknagl, Identification of p-wave superconductors, Phys. Rev. B **23**, 5788 (1981).
[3] C. Bruder, Andreev scattering in anisotropic superconductors, Phys. Rev. B **41**, 4017 (1990).
[4] C.-R. Hu, Midgap Surface States as a Novel Signature for $d^2_{xa} - x^2_b$-Wave Superconductivity, Phys. Rev. Lett. **72**, 1526 (1994).

[5] Y. Tanaka and S. Kashiwaya, Theory of Tunneling Spectroscopy of d-Wave Superconductors, Phys. Rev. Lett. **74**, 3451 (1995).
[6] S. Kashiwaya and Y. Tanaka, Tunnelling effects on surface bound states in unconventional superconductors, Rep. Prog. Phys. **63**, 1641 (2000).
[7] P. W. Anderson, Theory of dirty superconductors, J. Phys. Chem. Solids **11**, 26 (1959).
[8] A. V. Balatsky, I. Vekhter, and J.-X. Zhu, Impurity-induced states in conventional and unconventional superconductors, Rev. Mod. Phys. **78**, 373 (2006).
[9] A. P. Schnyder, S. Ryu, A. Furusaki, and A. W. W. Ludwig, Classification of topological insulators and superconductors in three spatial dimensions, Phys. Rev. B **78**, 195125 (2008).
[10] M. Sato, Topological properties of spin-triplet superconductors and Fermi surface topology in the normal state, Phys. Rev. B **79**, 214526 (2009).
[11] M. Sato, Topological odd-parity superconductors, Phys. Rev. B **81**, 220504 (2010).
[12] S. Ryu, A. P. Schnyder, A. Furusaki, and A. W. W. Ludwig, Topological insulators and superconductors: Tenfold way and dimensional hierarchy, New J. Phys. **12**, 065010 (2010).
[13] X.-L. Qi and S.-C. Zhang, Topological insulators and superconductors, Rev. Mod. Phys. **83**, 1057 (2011).
[14] T. Mizushima, Y. Tsutsumi, M. Sato, and K. Machida, Symmetry protected topological superfluid ^{3}He-B, J. Phys.: Condens. Matter **27**, 113203 (2015).
[15] B. Lu, P. Burset, Y. Tanuma, A. A. Golubov, Y. Asano, and Y. Tanaka, Influence of the impurity scattering on charge transport in unconventional superconductor junctions, Phys. Rev. B **94**, 014504 (2016).
[16] Ya. M. Blanter and M. Büttiker, Shot noise in mesoscopic conductors, Phys. Rep. **336**, 1 (2000).
[17] V. A. Khlus, Current and voltage fluctuations in microjunctions between normal metals and superconductors, Zh. Eksp. Teor. Fiz. **93**, 2179 (1987) [Sov. Phys. JETP **66**, 1243 (1987)]; B. A. Muzykantskii and D. E. Khmelnitskii, Quantum shot noise in a normal-metal–superconductor point contact, Phys. Rev. B **50**, 3982 (1994); M. J. M. de Jong and C. W. J. Beenakker, Doubled shot noise in disordered normal-metal–superconductor junctions, *ibid.* **49**, 16070 (1994).
[18] M. P. Anantram and S. Datta, Current fluctuations in mesoscopic systems with Andreev scattering, Phys. Rev. B **53**, 16390 (1996).
[19] P. Dieleman, H. G. Bukkems, T. M. Klapwijk, M. Schicke, and K. H. Gundlach, Observation of Andreev Reflection Enhanced Shot Noise, Phys. Rev. Lett. **79**, 3486 (1997).
[20] C. Kallin and J. Berlinsky, Chiral superconductors, Rep. Prog. Phys. **79**, 054502 (2016).
[21] A. P. Mackenzie and Y. Maeno, The superconductivity of Sr_2RuO_4 and the physics of spin-triplet pairing, Rev. Mod. Phys. **75**, 657 (2003); Y. Maeno, S. Kittaka, T. Nomura, S. Yonezawa, and K. Ishida, Evaluation of spin-triplet superconductivity in Sr_2RuO_4, J. Phys. Soc. Jpn. **81**, 011009 (2012); C. Kallin, Chiral p-wave order in Sr_2RuO_4, Rep. Prog. Phys. **75**, 042501 (2012).
[22] W. Huang, E. Taylor, and C. Kallin, Vanishing edge currents in non-p-wave topological chiral superconductors, Phys. Rev. B **90**, 224519 (2014); Y. Tada, W. Nie, and M. Oshikawa, Orbital Angular Momentum and Spectral Flow in Two-Dimensional Chiral Superfluids, Phys. Rev. Lett. **114**, 195301 (2015); T. Scaffidi and S. H. Simon, Large Chern Number and Edge Currents in Sr_2RuO_4, *ibid.* **115**, 087003 (2015).
[23] A. M. Black-Schaffer and C. Honerkamp, Chiral d-wave superconductivity in doped graphene, J. Phys.: Condens. Matter **26**, 423201 (2014).
[24] N. Read and D. Green, Paired states of fermions in two dimensions with breaking of parity and time-reversal symmetries and the fractional quantum Hall effect, Phys. Rev. B **61**, 10267 (2000).
[25] S. Fujimoto, Topological order and non-Abelian statistics in noncentrosymmetric s-wave superconductors, Phys. Rev. B **77**, 220501 (2008).
[26] J. D. Sau, R. M. Lutchyn, S. Tewari, and S. Das Sarma, Generic New Platform for Topological Quantum Computation Using Semiconductor Heterostructures, Phys. Rev. Lett. **104**, 040502 (2010); R. M. Lutchyn, J. D. Sau, and S. Das Sarma, Majorana fermions and a topological phase transition in semiconductor-superconductor heterostructures, *ibid.* **105**, 077001 (2010).
[27] M. Sato, Y. Tanaka, K. Yada, and T. Yokoyama, Topology of Andreev bound states with flat dispersion, Phys. Rev. B **83**, 224511 (2011); S. Kashiwaya, Y. Tanaka, M. Koyanagi, H. Takashima, and K. Kajimura, Origin of zero-bias conductance peaks in high-t_c superconductors, *ibid.* **51**, 1350 (1995).
[28] Y. Tanaka, Y. Mizuno, T. Yokoyama, K. Yada, and M. Sato, Anomalous Andreev Bound State in Noncentrosymmetric Superconductors, Phys. Rev. Lett. **105**, 097002 (2010); K. Yada, M. Sato, Y. Tanaka, and T. Yokoyama, Surface density of states and topological edge states in noncentrosymmetric superconductors, Phys. Rev. B **83**, 064505 (2011).
[29] J. You, C. H. Oh, and V. Vedral, Majorana fermions in s-wave noncentrosymmetric superconductor with Dresselhaus (110) spin-orbit coupling, Phys. Rev. B **87**, 054501 (2013).
[30] S. Ikegaya, Y. Asano, and Y. Tanaka, Anomalous proximity effect and theoretical design for its realization, Phys. Rev. B **91**, 174511 (2015).
[31] J. W. Serene and D. Rainer, The quasiclassical approach to superfluid ^{3}He, Phys. Rep. **101**, 221 (1983).
[32] J. Rammer and H. Smith, Quantum field-theoretical methods in transport theory of metals, Rev. Mod. Phys. **58**, 323 (1986).
[33] A. Millis, D. Rainer, and J. A. Sauls, Quasiclassical theory of superconductivity near magnetically active interfaces, Phys. Rev. B **38**, 4504 (1988).
[34] M. Ashida, S. Aoyama, J. Hara, and K. Nagai, Green's function in proximity-contact superconducting-normal double layers, Phys. Rev. B **40**, 8673 (1989).
[35] G. Eilenberger, Transformation of Gorkov's equation for type II superconductors into transport-like equations, Z. Phys. A **214**, 195 (1968).
[36] Y. Tanaka, Y. Tanuma, and A. A. Golubov, Odd-frequency pairing in normal-metal/superconductor junctions, Phys. Rev. B **76**, 054522 (2007).
[37] Y. Nagato, K. Nagai, and J. Hara, Theory of the Andreev reflection and the density of states in proximity contact normal-superconducting infinite double-layer, J. Low Temp. Phys. **93**, 33 (1993).
[38] N. Schopohl and K. Maki, Quasiparticle spectrum around a vortex line in a d-wave superconductor, Phys. Rev. B **52**, 490 (1995).
[39] A. Shelankov and M. Ozana, Quasiclassical theory of superconductivity: A multiple-interface geometry, Phys. Rev. B **61**, 7077 (2000).

[40] Y. Nagato and K. Nagai, Surface and size effect of a d_{xy}-state superconductor, Phys. Rev. B **51**, 16254 (1995).
[41] M. Matsumoto and H. Shiba, Coexistence of different symmetry order parameters near a surface in *d*-wave superconductors iii, J. Phys. Soc. Jpn. **65**, 2194 (1996).
[42] M. Eschrig, Distribution functions in nonequilibrium theory of superconductivity and Andreev spectroscopy in unconventional superconductors, Phys. Rev. B **61**, 9061 (2000).
[43] M. Fogelström, Josephson currents through spin-active interfaces, Phys. Rev. B **62**, 11812 (2000).
[44] E. Zhao, T. Löfwander, and J. A. Sauls, Nonequilibrium superconductivity near spin-active interfaces, Phys. Rev. B **70**, 134510 (2004).
[45] G. E. Blonder, M. Tinkham, and T. M. Klapwijk, Transition from metallic to tunneling regimes in superconducting microconstrictions: Excess current, charge imbalance, and supercurrent conversion, Phys. Rev. B **25**, 4515 (1982).
[46] J.-X. Zhu and C. S. Ting, Shot noise in a normal-metal–*d*-wave superconductor junction with a 110-oriented interface, Phys. Rev. B **59**, R14165 (1999).
[47] Y. Tanaka, T. Asai, N. Yoshida, J. Inoue, and S. Kashiwaya, Interface effects on the shot noise in normal-metal–*d*-wave superconductor junctions, Phys. Rev. B **61**, R11902 (2000).
[48] Y. Tanaka and A. A. Golubov, Theory of the Proximity Effect in Junctions with Unconventional Superconductors, Phys. Rev. Lett. **98**, 037003 (2007).
[49] F. S. Bergeret, A. F. Volkov, and K. B. Efetov, Long-Range Proximity Effects in Superconductor-Ferromagnet Structures, Phys. Rev. Lett. **86**, 4096 (2001); Odd triplet superconductivity and related phenomena in superconductor-ferromagnet structures, Rev. Mod. Phys. **77**, 1321 (2005); J. Linder, A. Sudbø, T. Yokoyama, R. Grein, and M. Eschrig, Signature of odd-frequency pairing correlations induced by a magnetic interface, Phys. Rev. B **81**, 214504 (2010); S. H. Jacobsen and J. Linder, Giant triplet proximity effect in π-biased Josephson junctions with spin-orbit coupling, *ibid.* **92**, 024501 (2015); I. Gomperud and J. Linder, Spin supercurrent and phase-tunable triplet Cooper pairs via magnetic insulators, *ibid.* **92**, 035416 (2015).
[50] Y. Tanaka, A. A. Golubov, S. Kashiwaya, and M. Ueda, Anomalous Josephson Effect Between Even- and Odd-Frequency Superconductors, Phys. Rev. Lett. **99**, 037005 (2007).
[51] T. Yokoyama, Josephson and proximity effects on the surface of a topological insulator, Phys. Rev. B **86**, 075410 (2012); A. M. Black-Schaffer and A. V. Balatsky, Odd-frequency superconducting pairing in topological insulators, *ibid.* **86**, 144506 (2012); F. Crépin, P. Burset, and B. Trauzettel, Odd-frequency triplet superconductivity at the helical edge of a topological insulator, *ibid.* **92**, 100507 (2015); P. Burset, B. Lu, G. Tkachov, Y. Tanaka, E. M. Hankiewicz, and B. Trauzettel, Superconducting proximity effect in three-dimensional topological insulators in the presence of a magnetic field, *ibid.* **92**, 205424 (2015); A. Aperis, P. Maldonado, and P. M. Oppeneer, *Ab initio* theory of magnetic-field-induced odd-frequency two-band superconductivity in MgB_2, *ibid.* **92**, 054516 (2015).
[52] B. Sothmann, S. Weiss, M. Governale, and J. König, Unconventional superconductivity in double quantum dots, Phys. Rev. B **90**, 220501 (2014); P. Burset, B. Lu, H. Ebisu, Y. Asano, and Y. Tanaka, All-electrical generation and control of odd-frequency *s*-wave cooper pairs in double quantum dots, *ibid.* **93**, 201402 (2016).
[53] A. M. Black-Schaffer and A. V. Balatsky, Odd-frequency superconducting pairing in multiband superconductors, Phys. Rev. B **88**, 104514 (2013); Y. Asano and A. Sasaki, Odd-frequency Cooper pairs in two-band superconductors and their magnetic response, *ibid.* **92**, 224508 (2015).
[54] Y. Tanaka, M. Sato, and N. Nagaosa, Symmetry and topology in superconductors—Odd-frequency pairing and edge states, J. Phys. Soc. Jpn. **81**, 011013 (2012).
[55] M. Eschrig, Spin-polarized supercurrents for spintronics: A review of current progress, Rep. Prog. Phys. **78**, 104501 (2015).
[56] N. V. Gnezdilov, B. van Heck, M. Diez, J. A. Hutasoit, and C. W. J. Beenakker, Topologically protected charge transfer along the edge of a chiral *p*-wave superconductor, Phys. Rev. B **92**, 121406 (2015).
[57] J. C. Cuevas, A. Martín-Rodero, and A. Levy Yeyati, Hamiltonian approach to the transport properties of superconducting quantum point contacts, Phys. Rev. B **54**, 7366 (1996).
[58] S. V. Bakurskiy, A. A. Golubov, M. Yu. Kupriyanov, K. Yada, and Y. Tanaka, Anomalous surface states at interfaces in *p*-wave superconductors, Phys. Rev. B **90**, 064513 (2014).
[59] E. Scheer, W. Belzig, Y. Naveh, M. H. Devoret, D. Esteve, and C. Urbina, Proximity Effect and Multiple Andreev Reflections in Gold Atomic Contacts, Phys. Rev. Lett. **86**, 284 (2001).
[60] A. Moor, A. F. Volkov, and K. B. Efetov, Excess current in ferromagnet-superconductor structures with fully polarized triplet component, Phys. Rev. B **93**, 174510 (2016).
[61] J. Wiedenmann, E. Bocquillon, R. S. Deacon, S. Hartinger, O. Herrmann, T. M. Klapwijk, L. Maier, C. Ames, C. Brüne, C. Gould, A. Oiwa, K. Ishibashi, S. Tarucha, H. Buhmann, and L. W. Molenkamp, 4π-periodic Josephson supercurrent in hgte-based topological Josephson junctions, Nat. Commun. **7**, 10303 (2016).
[62] E. S. Tikhonov, D. V. Shovkun, M. Snelder, M. P. Stehno, Y. Huang, M. S. Golden, A. A. Golubov, A. Brinkman, and V. S. Khrapai, Andreev Reflection in an *s*-Type Superconductor Proximized 3D Topological Insulator, Phys. Rev. Lett. **117**, 147001 (2016).
[63] Y. Tanaka and S. Kashiwaya, Anomalous charge transport in triplet superconductor junctions, Phys. Rev. B **70**, 012507 (2004); Y. Tanaka, S. Kashiwaya, and T. Yokoyama, Theory of enhanced proximity effect by midgap Andreev resonant state in diffusive normal-metal/triplet superconductor junctions, *ibid.* **71**, 094513 (2005).
[64] S. Ikegaya, S.-I. Suzuki, Y. Tanaka, and Y. Asano, Quantization of conductance minimum and index theorem, Phys. Rev. B **94**, 054512 (2016).
[65] Y. Asano and Y. Tanaka, Majorana fermions and odd-frequency Cooper pairs in a normal-metal nanowire proximity-coupled to a topological superconductor, Phys. Rev. B **87**, 104513 (2013).
[66] O. Kashuba, B. Sothmann, P. Burset, and B. Trauzettel, The Majorana stm as a perfect detector of odd-frequency superconductivity, Phys. Rev. B **95**, 174516 (2017).